Environmental Technology & Innovation 25 (2022) 102152

Contents lists available at ScienceDirect

Environmental Technology & Innovation

journal homepage: www.elsevier.com/locate/eti

# Harnessing biofertilizer from human urine via chemogenic and biogenic routes: Synthesis, characterization and agronomic application

Jayanta Kumar Biswas [a,b,*,1], Monojit Mondal [a,1], Dhrubajyoti Majumdar [c], Amit Bhatnagar [d], Binoy Sarkar [e], Meththika Vithanage [f], Erik Meers [g], Filip M.G. Tack [h], Deepak Pant [i], Ramesh Goel [j]

[a] *Enviromicrobiology, Ecotoxicology and Ecotechnology Research Laboratory, Department of Ecological Studies, University of Kalyani, Kalyani, Nadia 741235, West Bengal, India*
[b] *International Centre for Ecological Engineering, University of Kalyani, Kalyani 741235, West Bengal, India*
[c] *Department of Chemistry, Tamralipta Mahavidyalaya, Tamluk 721636, West Bengal, India*
[d] *Department of Separation Science, LUT School of Engineering Science, LUT University, Sammonkatu 12, FI 50130, Mikkeli, Finland*
[e] *Lancaster Environment Centre, Lancaster University, Lancaster, LA1 4YQ, United Kingdom*
[f] *Ecosphere Resilience Research Centre, Faculty of Applied Sciences, University of Sri Jayewardenepura, Nugegoda 10250, Sri Lanka*
[g] *Laboratory of Bioresource Recovery (RE-SOURCE LAB), Ghent University, Coupure Links 653, B-9000 Ghent, Belgium*
[h] *Department of Green Chemistry and Technology, Ghent University, Gent, Belgium*
[i] *Separation & Conversion Technology, Flemish Institute for Technological Research (VITO), Boeretang 200, 2400 Mol, Belgium*
[j] *Environmental Engineering and Microbiology Lab, Department of Civil & Environmental Engineering, University of Utah, Salt Lake City, United States*

ARTICLE INFO

*Article history:*
Received 30 July 2021
Received in revised form 12 November 2021
Accepted 19 November 2021
Available online 3 December 2021

*Keywords:*
Human urine
Resource recovery
Biomineralization
Struvite
Biofertilizer
Plant growth promotion

ABSTRACT

This study aimed at recovering nutrients from human urine as valorized products through chemical and biological mineralization, and assessing their fertilizer potential. Chemosynthesis of struvite ($MgNH_4PO_4{\cdot}6H_2O$) was accomplished from fresh human urine through chemical mineralization using magnesia, whereas biogenic synthesis was achieved through microbial mineralization by employing a wastewater bacterium (*Pseudomonas aeruginosa* KUJM KY355382.1). Elemental analysis and other characterization results confirmed the synthesized products as struvite under both chemical and biological synthesis methods. The potential of the chemogenic and biogenic struvite products as slow release fertilizer was reflected in improved plant growth characteristics, including height, fresh weight, dry weight, pod length and seed yield, of cowpea (*Vigna unguiculata*) compared to the control set. Specially, the seeds obtained per plant were 137.71 and 125.14% higher after application of chemogenic and biogenic struvite, respectively, compared to a no-fertilizer control. When assessing aging effect on struvite's chemical structure by comparing a 15-year old struvite crystal with the recently synthesized biomineral, the weathered struvite was found to lose $NH_4^+$ however, retain $PO_4^{3-}$ and $Mg^{2+}$, implying its phosphate supplying potential over a long period. Both the chemogenic and biogenic synthesis routes successfully converted human urine to fertilizer ('waste into wealth'), but the struvite yield was higher in the case of chemogenic synthesis using magnesia (474 ± 9.64 mg $L^{-1}$) than biogenic synthesis employing *Pseudomonas aeruginosa* KUJM (345 ± 6.08 mg $L^{-1}$). Still, the

* Correspondence to: Enviromicrobiology, Ecotoxicology and Ecotechnology Research Laboratory (3E-MicroToxTech Lab), Department of Ecological Studies & International Centre for Ecological Engineering, University of Kalyani, Kalyani, Nadia 741235, West Bengal, India.
*E-mail address:* jkbiswas@klyuniv.ac.in (J.K. Biswas).

[1] Authors contributed equally to this work.

https://doi.org/10.1016/j.eti.2021.102152

biogenic synthesis is preferred over the chemogenic route because the process is more eco-friendly.



## 1. Introduction

Wastewater generated from domestic, livestock, industrial and other anthropogenic sources is a mixture of organic matter, macro- and micro-elements such as nitrogen (N), phosphorus (P), potassium (K), calcium (Ca), and magnesium (Mg) (Onchoke et al., 2018), and potentially toxic elements (PTEs) (Ravndal et al., 2018). When discharged without or with little treatment, wastewater is a pollution source to the environment. High concentration of nutrients in wastewater, mainly arising from digestive and excretory wastes of humans and animals, if not managed appropriately, can trigger eutrophication-induced ecosystem degradation through harmful algal blooms and decline in the aquatic diversity (Carstea et al., 2016). To protect water quality and the ecosystem, wastewater effluents need to undergo efficient removal and recovery of nutrients prior to discharge into the environment following a circular economic approach (Biswas et al., 2020; Robles et al., 2020). The obvious driving factors for nutrient recovery and recycling through the circular economy are persistent resource (e.g. P) depletion, high energy intensity of conventional treatments, aging and decreasing efficiency of the existing wastewater treatment plants (WWTPs), and opportunity of wasted resources for recycling into the production cycle (Gherghel et al., 2019; Biswas et al., 2020).

Human urine (HU) represents a reservoir of multiple valuable and renewable nutrients: 10–12 g $L^{-1}$ N, 0.1–0.5 g $L^{-1}$ P, and 1.0–2.0 g $L^{-1}$ K, that contributes to the nutrient burden of municipal wastewater (Patel et al., 2020). Because it contains large amount of plant nutrients (N and P), HU has been successfully used as a biofertilizer in the cultivation of plants, emulating reuse and recycling as occurs with natural biogeochemical cycling of nutrients (Pandorf et al., 2018). Extracting the nutrient loads of urine prior to channeling it to the wastewater stream can significantly reduce the burden on wastewater treatment plants. This concept is gaining ground as a part of trends towards more sustainable ecological sanitation, resource recycling and the circular economy (Patel et al., 2020; Robles et al., 2020).

However, cultural taboos and moral prejudice of people in many countries including India have created a major mental 'stumbling block' and 'urine-blindness' which have limited the popularization of tapping the nutrient resource in HU and exploiting its nutrient recycling and energy recovery potential (Rana et al., 2017; Simha et al., 2018). Nevertheless, the environmental benefits of closing the enormous nutrient loop through application of HU in agriculture and/or aquaculture are clear. Therefore, safe and sound utilization of HU in organic production can open a window of opportunities to a large segment of poverty-stricken farmers living in the developing nations for opting for an inexpensive environment-friendly biofertilizer instead of costly and energy-intensive chemical fertilizers. This could help to achieve multiple United Nations Sustainable Development Goals (SDGs) such as SDG 2, SDG 3 and SDG 6, through food and agricultural security, and environmental health protection. Conversely, HU might contain pharmaceutical residues and pathogenic microorganisms, hence the application of raw urine to agricultural soils could be harmful to environmental and public health (Biswas et al., 2020). The storage and transportation of HU as fertilizer also become very challenging tasks. Separating urine at collection points before it enters the waste stream could enable the elimination of pathogens, and facilitate safe reuse of its valuable nutrients, especially N and P (Patel et al., 2020).

Different techniques have been employed to remove and recover nutrients from HU, mainly N compounds, P and Mg (Kabdaşlı and Tünay, 2018; Simha et al., 2018; Patel et al., 2020). Ammonia and phosphate have been removed from HU via precipitation as struvite ($NH_4MgPO_4{\cdot}6H_2O$), a mineral with very low solubility but high potential of being used as an excellent slow-release fertilizer in agriculture and horticulture (Kabdaşlı and Tünay, 2018). The notional constituents of struvite are N (5.7%), P (12.6%), and Mg (9.9%) with the remaining being water in crystalline state. Moreover, struvite has a lower load of trace contaminants and/or pathogenic microorganisms, while exhibiting a superior fertilizer (nutrient) potential per unit weight compared to organic waste streams (Uysal et al., 2010). As a P fertilizer, struvite is matched up favorably to mineral phosphates across a wide spectrum of soil pH (Kabdaşlı and Tünay, 2018; Chojnacka et al., 2020).

Struvite could be precipitated from HU via environmentally friendly microbial mineralization processes (biogenic struvite), avoiding the chemical processes (chemogenic struvite), which involve the use of harsh alkali reagents. Naturally occurring bacteria could precipitate struvite when microbial metabolism of nitrogenous compounds facilitates $NH_4^+$ release, and the consequent pH rise triggers the mineral precipitation reaction (Sinha et al., 2014). Urease and carbonic anhydrase enzymes secreted by certain bacterial strains catalyze the urea hydrolysis and subsequent struvite biomineralization extracellularly (Bhattacharya et al., 2018). Bacteria belonging to the genera *Azotobacter*, *Bacillus*, *Brevibacterium, Brucella*, *Flavobacterium*, *Halobacterium*, *Myxococcus*, *Proteus*, *Pseudomonas* and *Ureaplasma* have the ability to biomineralize struvite (Pratt et al., 2012; Soares et al., 2013; Gonzalez-Martinez et al., 2015). These bacterial strains occur in soils (e.g., *Myxococcus* sp., *Arthrobacter* sp., and *Pseudomonas* sp.) (Pratt et al., 2012), wastewater treatment plants (Gonzalez-Martinez et al., 2015), and other natural habitats (e.g., *Myxococcus xanthus*, *Acinetobacter calcoaceticus*, *Bacillus pumilus*, and *Brevibacterium antiquum*) (Soares et al., 2013). In fact, there is a close relationship between biomineralization of struvite and microbial growth and activities (González-Muñoz et al., 2010).

Although considerable studies have been conducted on struvite recovery from wastewater using chemical approaches, microbial mineralization has been scarcely adopted. There is a paucity of information on comparative assessment of fertilizer potentials of chemogenic and biogenic struvite produced from HU, and their application to soils for agricultural crop production. To the best of the authors' knowledge, weathering or aging effect of struvite crystals on their chemical constituents and nutrient potential (agronomic value) has never been assessed. To fill these knowledge gaps, this study was conducted with the following objectives: (1) synthesize biofertilizer from HU following both chemogenic and biogenic (involving bacteria) routes; (2) characterize the crystalline structure and physicochemical properties of the valorized product; (3) assess aging effect on the mineral's crystal structure particularly its nutrient potential by comparing a 15-year old struvite crystal with the recently synthesized biomineral; and (4) evaluate the fertilizer potential of both chemogenic and biogenic struvite for prospective application in agriculture.

## 2. Materials and methods

### 2.1. Source of urine

Fresh HU was obtained from the toilet used by healthy and unmedicated male students of the age group of 23–25 years of the Department of Ecological Studies, Kalyani University, West Bengal, India. The HU samples were collected from individuals in aseptic conditions adopting all the precautions such as sterile container, mask, gloves, clean toilet, etc.

### 2.2. Biomineral synthesis from HU using chemogenic method

To produce magnesia, 1 g of magnesium chloride ($MgCl_2 \cdot 6H_2O$) and 1 g of ammonium chloride ($NH_4Cl$) were dissolved in 5 mL of distilled water, then 0.5 mL of concentrated ammonium hydroxide solution (35% $NH_4OH$) was added and diluted up to 10 mL with distilled water. Using this magnesia solution, chemogenic mineral was synthesized as follows: in a 1 L conical flask, 750 mL of fresh HU was taken and 10 mL of magnesia solution was added. The conical flask was cotton plugged and stored for 10 days without shaking at room temperature. The set without any addition of magnesis was maintained as control. After 10 days the liquid was decanted carefully and the precipitated mineral crystals were washed three times with methanol, then air dried and stored for further analysis. In the control sets, no precipitation of mineral crystals was observed.

### 2.3. Biomineral synthesis from HU using biogenic method

In case of the biogenic mineral synthesis, a wastewater bacterium (*Pseudomonas aeruginosa* KUJM KY355382.1) previously isolated by our group (Biswas et al., 2017) from the grit chamber of the Kalyani city's wastewater treatment plant (Kalyani, West Bengal, India) was used. As a starter culture, *P. aeruginosa* was grown in 10 mL glucose minimal salt media. A volume of 750 mL fresh HU was put in a 1 L conical flask and 10 mL of overnight grown *P. aeruginosa* culture was added. The flask was cotton plugged and incubated at 37 °C for 10 days without shaking. The control set was maintained without adding any bacterial inoculation. After 10 days, the solid mineral was collected as stated earlier. In the control set, no mineral crystal was precipitated.

### 2.4. Characterization of the synthesized minerals

Elemental analysis (P, H, and N) of chemogenic mineral was performed with a Perkin–Elmer CHN analyzer (Model 2400). Fourier transform infrared (FT-IR) spectra were recorded as KBr pellets in the wavenumber range of 4000–400 $cm^{-1}$ with 16 scans at a resolution of 4 $cm^{-1}$ on a Perkin–Elmer spectrum RX 1 instrument where a deuterated triglycine sulfate (DTGS) detector was used. The FT-Raman spectra were obtained by means of a Bruker RFS 27 Stand-alone FT-Raman spectrometer in the scan range of 50–4000 $cm^{-1}$ and a resolution of 2 $cm^{-1}$. The proton nuclear magnetic resonance ($^1H$ NMR) spectra of the mineral compounds were collected at room temperature using a Bruker DPX-400 MHz NMR spectrometer in dimethyl sulfoxide (DMSO) solvent. The powder X-ray diffraction (PXRD) patterns of the mineral samples were acquired on a Bruker D8 Advance X-ray diffractometer with Cu K$\alpha$ radiation ($\alpha = 1.548$ Å) generated at 40 kV and 40 mA. The XRD patterns were recorded in a $2\theta$ range of 5–50° using 1-D Lynxeye detector at ambient conditions.

The single crystal data of the synthesized minerals were collected on a Bruker SMART CCD (Sheldrick, SADABS) diffractometer (Mo K$\alpha$ radiation, $\lambda = 0.71073$ Å). The program SMART was utilized for collecting frames of data, indexing reflections and determining lattice factors, whereas SAINT (SMART & SAINT, Ver. 6.45) for integration of the intensity of reflections and scaling, SADAB (SHELXTL Ver. 6.1) for absorption correction, and SHELXTL for space group and structure determination and least-squares refinements on F2. The crystal structure of the mineral was fully solved and refined by full-matrix least-square methods against F2 using the program SHELXL-2014 (Sheldrick, SHELXTL Ver. 6.12) with Olex-2 software (Bradenburg, Diamond, Ver. 3.1eM; Dolomanov et al., 2009). All different atoms of struvite except hydrogen were refined with anisotropic displacement parameters. Hydrogen positions were set at calculated positions and refined isotopically.

### 2.5. Mesocosm study

Fertilizer potential of the synthesized chemogenic and biogenic minerals was tested on cowpea (*Vigna unguiculata*, variety: BCCP-3) plants. The soil (1 kg $pot^{-1}$; pH 4.99, electrical conductivity 135 $\mu S\ cm^{-1}$, $NO_3$–N concentration 31.14 mg $kg^{-1}$, $NH_4$–N concentration 8.21 mg $kg^{-1}$ and available P 6.82 mg $kg^{-1}$) used in the study was collected from a grassland area of the Kalyani University campus (22.9862°N, 88.4464°E). The experiment was conducted with five sets of treatments designated as chemogenic struvite (Cg), biogenic struvite (Bg), soluble P source (SP), insoluble P source (IP) and control (C); without any extraneous nutrient input). For each Bg and Cg treatment, 100 mg $kg^{-1}$ of synthesized biogenic or chemogenic mineral was blended with the soil. The soil of SP treatment received 50 mg $kg^{-1}$ of soluble phosphate (as $KH_2PO_4$), while the soil of IP received 100 mg $kg^{-1}$ of phosphate in precipitated form ($Ca_3(PO_4)_2$). All the treatments were maintained in triplicates and kept in a net house. The pots were sprinkled with an adequate quantity of water to maintain the soil moisture level at field capacity while preventing any leaching of surplus water. The pots were kept for three days for stabilization of the system before sowing the cowpea seeds. Two surface sterilized cowpea seeds were sown per pot. Seed germination took four days. The experiment lasted for 60 days.

Selected soil parameters were analyzed at three stages of the plant growth experiment: initially at day 1, in the middle at 30 days after seed sowing, and finally 60 days after seed sowing at the plant harvest. The soil pH and electrical conductivity (EC) were monitored with an electrode where soil: water ratio was maintained at 1:2.5 and 1:2, respectively. The $NO_3$–N and $NH_4$–N of the soil were extracted by 2*M* KCl and subsequently measured (Keeney and Nelson, 1982). Soil available P was extracted by sodium bicarbonate and measured using standard protocol (Olsen et al., 1954). The acid phosphatase and alkaline phosphatase activity of the soil were examined using sodium p-nitrophenyl phosphate as substrate and modified universal buffer at pH 6.5 (for acid phosphatase) and pH 11 (for alkaline phosphatase) (Tabatabai and Bremner, 1969; Piotrowska-Długosz and Wilczewski, 2014). These soil parameters were monitored on day 1 (initial), 30 (middle) and 60 (final).

On day 30, the number of leaves was counted and chlorophyll content was measured by extracting chlorophyll from leaves with solvents followed by spectrophotometric determination (Fridgen and Varco, 2004). Harvesting of plants was done on day 60, and different plant growth traits, namely plant height, fresh weight, dry weight, pod length and number of seeds per plant were recorded.

### 2.6. Statistical analyses

The data obtained were statistically analyzed using GraphPad Prism 7.0 software (GraphPad Software, USA). Two-way ANOVA was performed for plant growth related parameters. Treatment differences were verified by the Least Significant Difference (LSD) test at $P < 0.05$ level. Linear regression analyses between related parameters such as phosphatase enzyme and phosphate concentrations were performed. The level of statistical significance was accepted at $P < 0.05$.

## 3. Results and discussion

### 3.1. Characterization of the synthesized mineral

#### 3.1.1. Bulk crystal structure

A synopsis of the crystallographic data and structure refinement parameters of the minerals is presented in Table 1. The PXRD pattern of chemogenic mineral intimately resembled that of the biogenic mineral samples [Supplementary Information]. The crystallographic data (excluding structure factors) of the mineral samples were deposited to the Cambridge Crystallographic Data Centre as supplementary publication no. CCDC 1843500. The copies of the data can be obtained without any charge, on application to CCDC, 12 Union Road, Cambridge CB2 1EZ, U.K.: http://www.ccdc.cam.ac.uk/cgi-bin/catreq.cgi, e-mail: data_request@ccdc.cam.ac.uk, or fax: +44 1223 336033.

The experimental PXRD patterns of the bulk mineral samples were in close conformity with the simulated XRD patterns from single crystal X-ray diffraction, confirming the purity of the bulk samples. The yield of mineral synthesized involving biogenic and chemogenic systems were 345 ± 6.08 and 474 ± 9.64 mg $L^{-1}$, respectively.

#### 3.1.2. Single crystal structure

Full crystallographic data and detailed structural refinement parameters for the synthesized mineral are presented in Table 1. Selected crystallographic bond parameters and bond angles are summarized in Table 2. The mineral had crystallized in the orthorhombic space group Pmn21. The asymmetric unit (Fig. 1a) consisted of one magnesium atom, with half occupancy, coordinated to four water molecules, one phosphate group with half occupancy and one ammonium ion with half occupancy.

From the structural elucidation, the biomineral synthesized was identified as struvite. In the full structure (Fig. 1b), one bivalent magnesium ion, hexa-coordinated by six water molecules, adopted distorted octahedral geometry, as $[Mg(H_2O)_6]^{2+}$ was observed. The water molecule O1 and O2 occupied axial positions and O3, O3a, O4 and O4a {Mg1–O1 = 2.10 Å, Mg1–O2 = 2.13 Å, Mg1–O3 = 2.08 Å, Mg1–O3a = 2.08 Å, Mg1–O4 = 2.04 Å, Mg1–O4a = 2.04 Å, a = symmetry equivalent} occupied the equatorial plane. A close inspection of the crystal structure of struvite revealed that all the bond

**Table 1**
Summary of crystal data and full structure refinement parameters for the biomineral (struvite).

| | |
|---|---|
| Formula | $H_{16}MgNO_{10}P$ |
| M/g | 245.42 |
| Crystal system | Orthorhombic |
| Space group | *P m n 21* |
| *a*/Å | 6.9601(17) |
| *b*/Å | 6.1522(14) |
| *c*/Å | 11.244(3) |
| $\beta$ (°) | 90 |
| *V*/Å$^3$ | 481.5(2) |
| *Z* | 2 |
| $\rho_c$/g cm$^{-3}$ | 1.693 |
| $\mu$/mm$^{-1}$ | 0.386 |
| *F* (000) | 260 |
| Crystal size (mm$^3$) | 0.24 × 0.21× 0.18 |
| $\theta$ range (°) | 3.31 to 28.33 |
| Limiting indices | $-7 \le h \le 9$<br>$-8 \le k \le 8$<br>$-11 \le l \le 14$ |
| Reflns collected | 5423 |
| Ind reflns | 1147[$R_{int} = 0.0448$, $R_{sigma} = 0.0688$] |
| Completeness to $\theta$ (%) | 99.00 |
| Refinement method | Full-matrix-block least-squares on $F^2$ |
| Data/restraints/parameters | 1147/13/103 |
| Goodness-of-fit on $F^2$ | 1.157 |
| Final *R* indices | $R_1 = 0.0283$ |
| [$I > 2\theta(I)$] | $wR_2 = 0.0686$ |
| R indices (all data) | $R_1 = 0.1060$ |
| | $wR_2 = 0.0943$ |
| Largest diff. peak and hole (e Å$^{-3}$) | 1.182 and −2.215 |
| CCDC number | 1 843 500 |

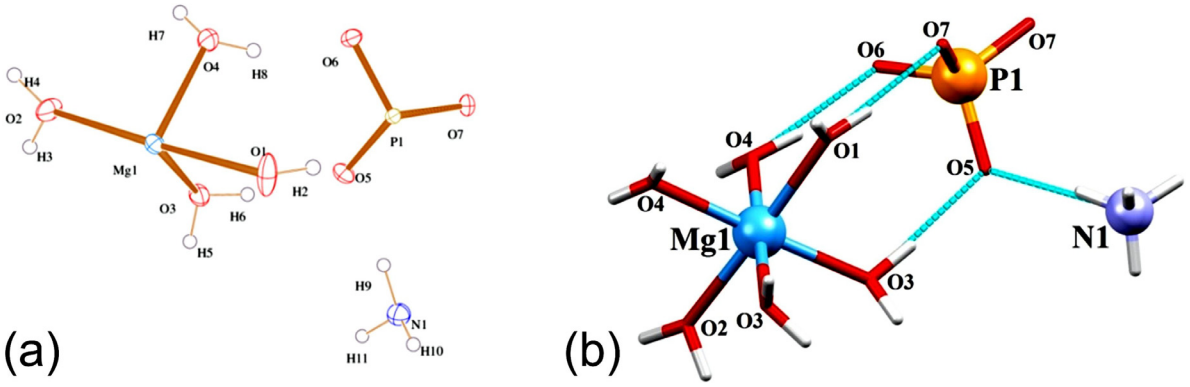


**Fig. 1.** Asymmetric unit (a) and full structure (b) of the mineral synthesized from human urine.

distance and bond angles were similar and comparable with values reported in the literature (Table 3) (Trobajo et al., 2007; Weil, 2008; Yang et al., 2014). The phosphate group and ammonium ion adopted distorted tetrahedral geometry. Although there was no covalent bond between the three moieties, an extensive hydrogen bonding (H-bonding) interaction among them was observed (Figs. 2, 3, and 4).

The $[Mg(H_2O)_6]^{2+}$ moiety was hydrogen bonded with four phosphate groups and two ammonium ions (Fig. 2). The two hydrogens ($H_2$) of water molecule O1 were H-bonded with O7 of two symmetry related phosphate groups. The hydrogen (H3) of O2 molecule was H-bonded with O6 of another phosphate group. The two-symmetry related water molecules O3 were H-bonded in trifurcated fashion with O5 and O7 of phosphate group and with the hydrogen atom of ammonium ion. Other two symmetry related water molecules O4 were H-bonded with O6 and O7 of the phosphate groups. The ammonium moiety $[NH_4]^+$ was hydrogen bonded (Fig. 3) by two $[Mg(H_2O)_6]^{2+}$ groups and one phosphate group. The hydrogen atoms H10 of N1 were H-bonded with the oxygen of the two symmetry related water molecules O3 and another hydrogen atom H9 of N1 was H-bonded with the O5 of the phosphate group.

The phosphate moiety was H-bonded with six $[Mg(H_2O)_6]^{2+}$ groups and one ammonium ion. All the four oxygen of the phosphate group formed H-bond in trifurcated fashion with hydrogen of the water molecules and ammonium ion.

**Table 2**
Selected bond distances (Å) and bond angles (°) for the biomineral (struvite).

| Bond Lengths around Mg(II) | | Bond angles around Mg(II) | |
|---|---|---|---|
| Mg(1)–O(1) | 2.100(1) | H(2)–O(1)–Mg(1) | 120.00(0) |
| Mg(1)–O(2) | 2.129(1) | H(2)–O(1)–H(2) | 119.00(0) |
| Mg(1)–O(3) | 2.078(1) | H(3)–O(2)–H(4) | 94.00(0) |
| Mg(1)–O(4) | 2.044(1) | H(3)–O(2)–Mg(1) | 115.00(0) |
| O(5)–P(1) | 1.548(0) | H(4)–O(2)–Mg(1) | 151.00(0) |
| O(6)–P(1) | 1.545(0) | H(5)–O(3)–Mg(1) | 122.00(0) |
| O(7)–P(1) | 1.542(0) | H(6)–O(3)–Mg(1) | 119.00(0) |
| H(9)–N(1) | 0.970(1) | H(7)–O(4)–Mg(1) | 114.00(0) |
| H(10)–N(1) | 0.960(1) | Mg(1)–O(4)–H(8) | 109.50(0) |
| H(11)–N(1) | 0.950(1) | Mg(1)–O(3)–H(5) | 122.000(0) |
| H(2)–O(1) | 0.850(1) | Mg(1)–O(3)–H(6) | 119.00(0) |
| H(3)–O(2) | 0.870(1) | Mg(1)–O(4)–H(7) | 114.000(0) |
| H(4)–O(2) | 0.870(1) | Mg(1)–O(4)–H(8) | 109.50(0) |
| H(5)–O(3) | 0.860(5) | O(5)–P(1)–O(6) | 109.80(0) |
| H(7)–O(4) | 0.730(9) | O(5)–P(1)–O(7) | 109.70(0) |
| | | O(6)–P(1)–O(7) | 108.60(0) |
| | | O(7)–P(1)–O(7) | 110.30(0) |
| Bond angles around Mg(II) | | | |
| O(1)–Mg(1)–O(2) | 177.5(0) | | |
| O(1)–Mg(1)–O(3) | 90.00(0) | | |
| O(1)–Mg(1)–O(4) | 88.80(0) | | |
| O(2)–Mg(1)–O(3) | 91.80(0) | | |
| O(2)–Mg(1)–O(4) | 89.40(0) | | |
| O(3)–Mg(1)–O(4) | 87.30(0) | | |
| O(3)–Mg(1)–O(3) | 93.60(0) | | |
| O(3)–Mg(1)–O(4) | 178.4(0) | | |
| O(4)–Mg(1)–O(4) | 91.70(0) | | |
| O(3)–Mg(1)–O(4) | 87.30(0) | | |

**Table 3**
Comparative survey of [Mg–O] and [O–P] bond distances (Å) of the synthesized chemogenic biomineral (struvite) with other reported struvite analogue compounds.

| Synthesized chemogenic struvite sample (present study) | Bond distances (Å) | Struvite analogue $KNiPO_4 \cdot 6H_2O$ sample (1) | $NH_4$-analog of hazenite struvite sample (2) | Struvite analogue $Cs[Mg(OH_2)6](PO_4)$ sample (3) |
|---|---|---|---|---|
| 2.100(1) | Mg-O | 2.251(1) | 2.032(3) | 2.054(4) |
| 2.129(1) | | 2.1807(8) | 2.040(3) | 2.082(3) |
| 2.078(1) | | 2.101(9) | 2.066(2) | |
| 2.044(1) | | 2.156(2) | 2.083(2) | |
| | | 2.131(1) | 2.060(2) | |
| | | 2.138(2) | 2.074(2) | |
| | | | 2.042(3) | |
| | | | 2.046(3) | |
| | | | 2.095(2) | |
| | | | 2.077(2) | |
| 1.548 | P-O | 1.508(1) | 1.544(3) | 1.536(3) |
| 1.545 | | 1.5424(8) | 1.548(3) | 1.539(6) |
| 1.542 | | 1.5254(6) | 1.540(3) | |
| | | 1.582(2) | 1.544(3) | |
| | | | 1.530(2) | |
| | | | 1.538(2) | |
| | | | 1.536(3) | |
| | | | 1.537(3) | |

The interactions are shown in Fig. 4. This type of hydrogen bonding feature is very much identical with already reported struvite analogue compounds (Trobajo et al., 2007; Weil, 2008). Because of such type of H-bonding, the mineral formed a three-dimensional network in the solid-state and the three units were held tightly in the crystal packing.

A comparison was made between an aged crystal structure of struvite and recently synthesized struvite. The weathered sample of struvite was about 15 years older than the newly synthesized struvite samples used in the present study. The old struvite sample was prepared by the chemogenic method as described earlier, and stored in a non-airtight container at room temperature to allow weathering of the mineral. An interesting crystal structure topology was observed in this respect. The old struvite sample reflected a crystal structure of central $Mg^{2+}$ coordinated by water molecules, but $NH_4^+$ was completely removed from the structure. Besides, the crystal structure of fresh struvite sample had a $Mg^{2+}$ coordinated with only half occupancy of a phosphate group which in the old sample crystal was fully retained. In this respect, we compared the mass spectrum between old and fresh sample of struvite [Supplementary Information]. It was observed

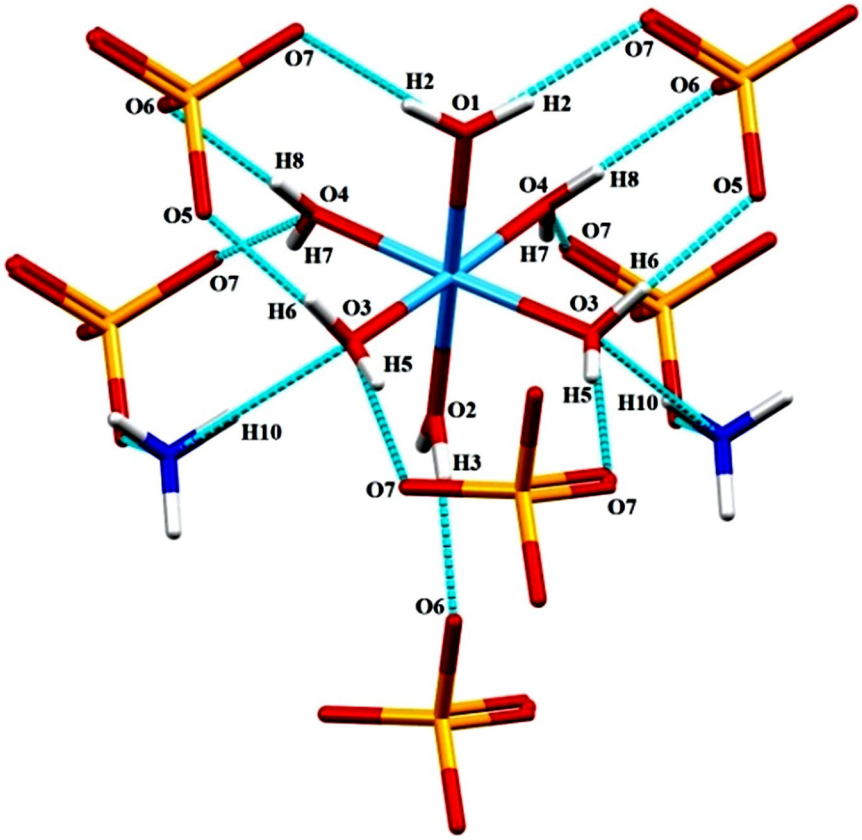


**Fig. 2.** Bonding interactions among constituents and symmetry observed in the mineral synthesized from human urine.

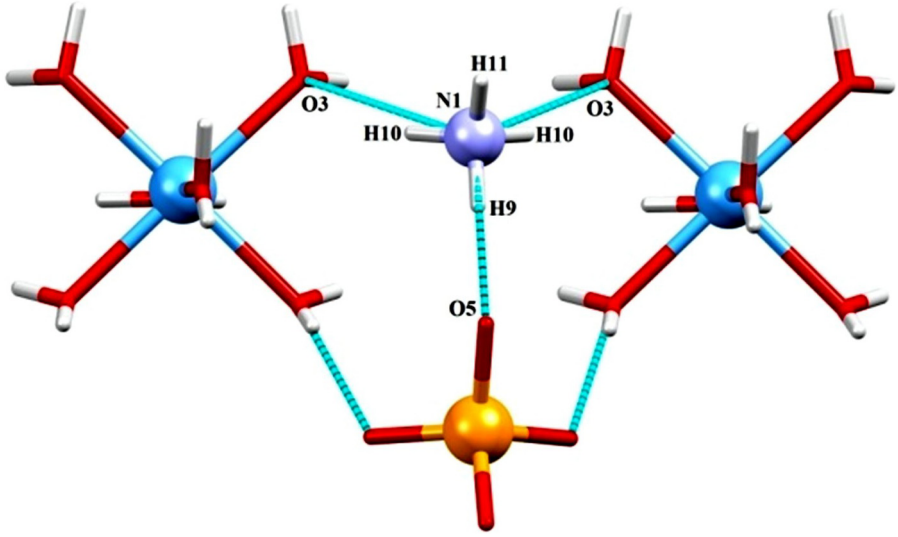


**Fig. 3.** Hydrogen bonding to maintain the ammonium moiety of the mineral synthesized from human urine.

that although the recovery of $NH_4^+$ from the old struvite sample was difficult after a long time, phosphate retained in the crystal structure was easily recoverable. It suggested that struvite retained its phosphate fertilizing potential for a longer period than its N fertilizing capacity, which bears an important agronomic connotation.

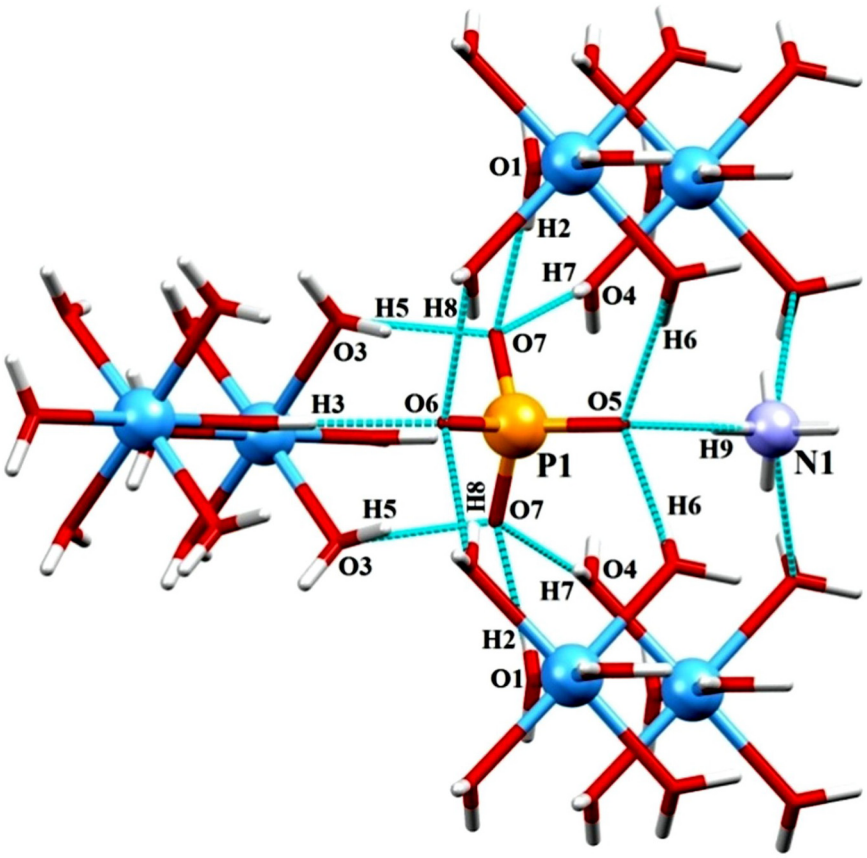


**Fig. 4.** Hydrogen bonding to maintain the phosphate moiety of the mineral synthesized from human urine.

The chemical formula of chemogenic struvite derived from its elemental analysis fitted well with calculated and experimental values. The calculated (expected) values for elemental analyses for H16MgNO10P: H 2.57; N 5.71, Mg 9.90, P 12.62 corresponded closely with the experimentally observed values: H 2.51; N 5.62, Mg 9.85, P 12.45. These also matched with the biogenic and other kind of struvite compounds.

In chemo- and biogenic struvite, central $Mg^{2+}$ was strongly coordinated by water molecules and half occupancy of $PO_4^{3-}$ group as well as $NH_4^+$. The FT-IR and FT-Raman spectra were investigated to establish such coordination environment. In the FT-IR spectra, the stretching mode region of the water molecules and ammonium ions gave a broad asymmetric band at 3430 $cm^{-1}$. This also supported the existence of hydrogen bonds in the crystal structure of chemogenic struvite. This observation was very much identical with the biogenic struvite sample [Supplementary Information]. The spectral position was in close proximity with other struvite compounds such as magnesium ammonium phosphate hexahydrate or MNP ($MgNH_4PO_4{\cdot}6H_2O$), magnesium potassium phosphate hexahydrate or MKP ($MgKPO_4{\cdot}6H_2O$) and arsenstruvite or magnesium ammonium arsenate hexahydrate or MNA ($MgNH_4AsO_4{\cdot}6H_2O$) spectra (Cahil et al., 2007). The similarity of the IR spectral signature in case of the ammonium compounds compared to the spectra of the potassium analogues (Stefov et al., 2013) implied that the main contribution was owed to the intensity of the bands in the O–H/N–H bonds. For the IR spectrum of struvite, the most thorough band at 1632 $cm^{-1}$ could perhaps be credited to d(HOH) vibrations or to modes having a substantial d(HOH) character. The band near 1466 $cm^{-1}$ could be attributed to the $\nu 4(NH_4)$ modes. In the region of the external vibrations of water molecules and ammonium ions, bands appeared at 1272–1216 $cm^{-1}$. This IR spectral value was very close to NiNP and NiKP types of struvite (Ferraris et al., 1986). A strong, slightly asymmetric and thermo-sensitive band emerged above 1071–1002 $cm^{-1}$ in the region of $\nu 3(PO_4)$ mode.

Typical Raman spectra of chemogenic struvite displayed three main bands at 943 $cm^{-1}$, 454 $cm^{-1}$ and 562 $cm^{-1}$ attributed to the $\gamma 1$, $\gamma 2$ and $\gamma 4$ $PO_4^{3-}$ benching modes [Supplementary Information] (Angoni et al., 1998). The Raman spectra of the struvite also showed a band at 292 $cm^{-1}$, which was assigned to the Mg–O stretching vibration. FT-Raman spectra of chemogenic struvite were identical with the biogenic struvite and other harvested struvite samples (Frost et al., 2005).

The $^1H$ NMR spectrum of 5 mg $mL^{-1}$ chemogenic struvite suspended in DMSO-d6 indicated the main peak at 3.34 ppm, which confirmed the presence of water released from struvite compound. The singlet at 2.50 ppm indicated

that ammonium was present in the struvite compound. Again, the $^1$H NMR spectra of the biogenic struvite were totally identical with the chemogenic struvite [Supplementary Information]. Mass spectrum (e/m 244) of the chemogenic struvite further confirmed the molecular mass of the struvite compound [Supplementary Information].

### 3.2. Mesocosm experiment findings

#### 3.2.1. Soil pH and EC

Soil pH ranged between 4.98–6.89, 4.92–7.09, 4.98–6.91, 4.99–6.90 and 5.12–6.78 in Bg, Cg, SP, IP and C, respectively. Soil pH showed an increasing trend with time in all sets registering significant differences ($P < 0.05$) among days of observation (Fig. 5a), although no significant difference ($P > 0.05$) in pH was shown among the treatments. Soil EC varied as 132.8–75.57, 139.40–82.80, 137.67–69.87, 128.30–71.50 and 122.37–49.90 $\mu$S cm$^{-1}$ in Bg, Cg, SP, IP and C, respectively, showing a gradually declining trend (Fig. 5b). Significantly treatment differences in EC values were observed for Bg and Cg from other treatments in the middle and at the end of the experiment.

#### 3.2.2. Nitrate-N

Nitrate–N concentrations in soil varied as 6.16–32.63, 6.08–32.95, 2.3–29.72, 2.4–29.06 and 2.37–29.32 mg kg$^{-1}$ in Bg, Cg, SP, IP and C, respectively. Both Bg and Cg showed significantly higher $NO_3$–N concentrations (11.28–160.23%) than other treatments (SP, IP and C). Two distinct groups: (Bg, Cg) and (SP, IP, C) with no significant differences between the group members were found (Fig. 5c). Soil $NO_3$–N decreased significantly ($P < 0.05$) with time in all the treatments.

#### 3.2.3. Ammoniacal-N

The $NH_4$–N concentrations in soil of Bg and Cg ranged between 6.02 to 9.32 mg kg$^{-1}$ which were markedly higher than that of other treatments (SP, IP and C) with concentration range of 3.61 to 7.19 mg kg$^{-1}$. The $NH_4$–N in soil decreased significantly ($P < 0.05$) in Bg and Cg till day 30 followed by a nearly steady state with no significant ($P > 0.05$) decline recorded. Conversely, in SP, IP and C, $NH_4$–N concentrations decreased significantly throughout the period of experiment (Fig. 5d). The $NH_4$–N concentrations in Bg and Cg were noticed as 30.54, 23.55% higher at day 1 than that in the control, which increased further by 80.79, 64.79% respectively on the final day (day 60) of observation.

#### 3.2.4. Available-P

The overall mean concentrations of available-P in soil were found to be 4.87, 5.05, 4.49, 3.71 and 3.52 mg kg$^{-1}$ in Bg, Cg, SP, IP and C, respectively. At the beginning (day 1), available-P concentrations of soil showed no significant difference ($P > 0.05$) among the treatments. During day 30–60, both Bg and Cg showed consistently higher available-P concentrations than SP, IP and C although no significant differences ($P > 0.05$) were shown between Bg and Cg, and SP and IP (Fig. 5e).

#### 3.2.5. Chlorophyll

There appeared no significant differences ($P > 0.05$) in leaf chlorophyll (a, b and total) contents among Bg Cg and SP systems, which were significantly ($P < 0.05$) higher than those in IP and C (Fig. 5f). Bg and Cg showed 58 to 62% higher concentrations of total chlorophyll compared to the control.

#### 3.2.6. Acid and alkaline phosphatase activity

In all systems, acid phosphatase activity was found to be higher than the alkaline phosphatase activity. During the course of investigation, acid and alkaline phosphatase activities in Bg and Cg were recorded as respectively 26.83–48.65 and 60.67–124.68% higher than those in C. Acid phosphatase activities increased significantly ($P < 0.05$) with time in all systems (Fig. 5g). While Bg, Cg and SP revealed an increase in alkaline phosphatase activity throughout, IP and C exhibited a significant increase after day 30 only (Fig. 5h). For both acid and alkaline phosphatase activity, there appeared two distinct groups comprising Bg, Cg and SP showing significantly higher concentrations than IP and C till day 30. Thereafter the same trend (Bg, Cg, SP > IP, C) continued for acid phosphatase activity but significant variations were observed in alkaline phosphatase activities among the treatments showing the following order Cg > Bg > SP > IP > C.

Plant growth related parameters studied are presented in Table 4. No significant variation ($P > 0.05$) was noticed in plant height among the treatments. Average number of leaves per plant recorded was the highest in Bg followed by SP and Cg which were 33.33, 25.93 and 18.52%, higher than that in the control. Similarly, on harvest fresh weights of the plants grown in Bg, Cg and SP registered 67.89, 63.35, 47.53%, higher over the control system. Similar pattern was observed for average pod length being 48.14, 37.83 and 25.57% longer in Bg, Cg and SP respectively relative to that in the control. There was no significant difference in number of seeds produced among Bg, Cg and SP, which were 109.57 to 137.50%, higher than the control.

The concentrations of $NO_3$–N and $NH_4$–N in the treatments containing biogenic and chemogenic struvite were consistently higher than the control as well as the systems treated with soluble-P or insoluble-P. This is due to the fact that struvite being the mineral containing $NH_4$–N contributed higher concentrations of the inorganic nitrogen species in both struvite-treated sets compared to other systems which received no extraneous input of nitrogenous nutrient.

Many studies reported that struvite is a slow release fertilizer (Talboys et al., 2016). The solubility of struvite is 1-10 mM at pH < 5 (Abbona et al., 1982), and in soil with acidic to neutral pH condition, its solubility ranges from 65 to

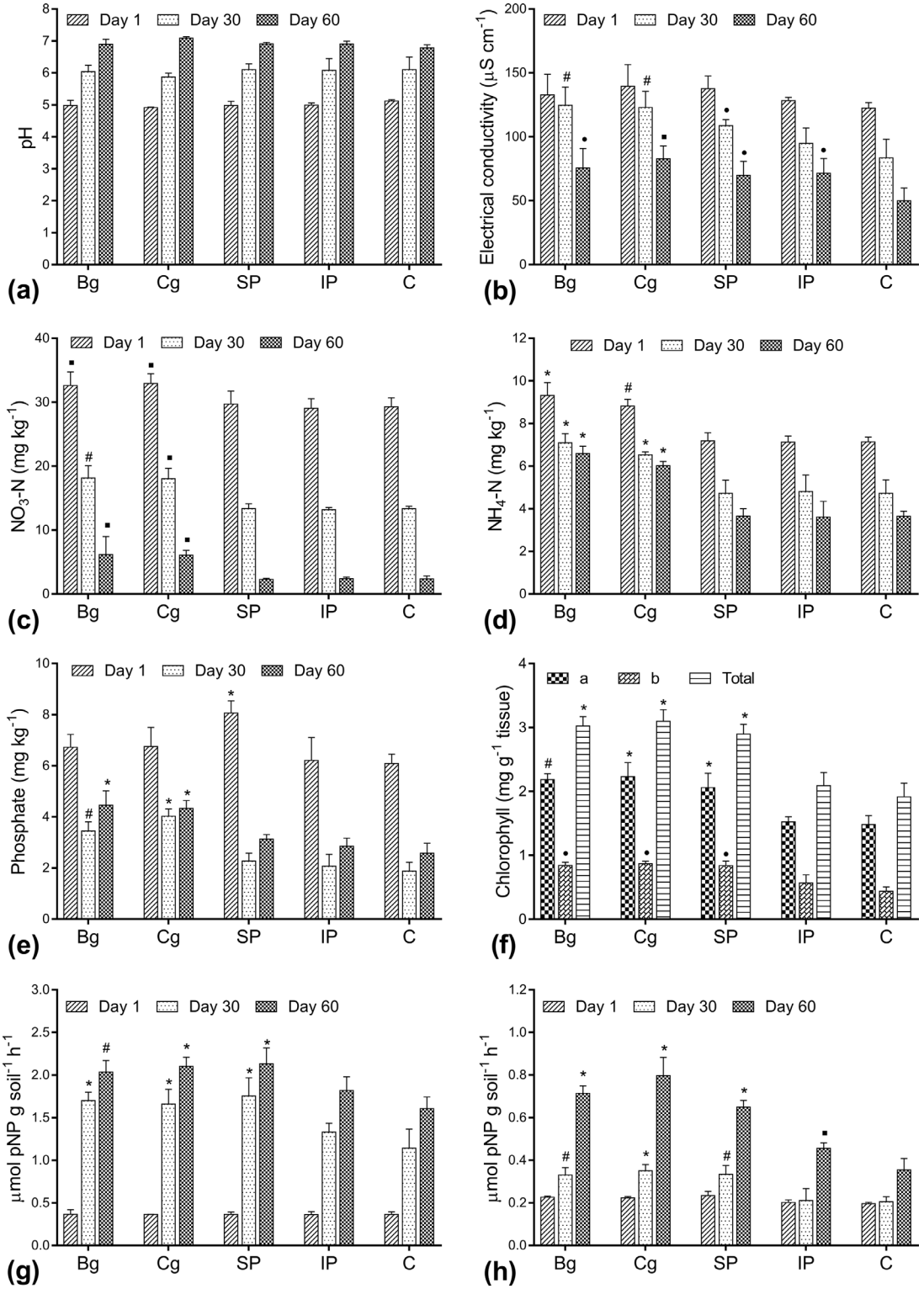


**Fig. 5.** Soil (a) pH, (b) electrical conductivity, (c) $NO_3$–N, (d) $NH_4$–N, (e) available-P, (f) leaf chlorophyll content, (g) acid phosphatase activity, and (h) alkaline phosphatase activity. Here Bg, Cg, SP, IP and C designated as biogenic, chemogenic, soluble-P, insoluble-P and control, respectively. Significant differences compared to respective control are marked with * for $P < 0.0001$; # for $P < 0.001$; ■ for $P < 0.01$; ● for $P < 0.05$; as derived from statistical analysis using two-way ANOVA followed by LSD.

**Table 4**
Effect of exogenous introduction of struvite, soluble-P and insoluble-P on morphological features of cowpea (*Vigna unguiculata*, variety: BCCP-3) plant. Each value indicates the mean of triplicate measurements ± standard deviation. Significant differences compared to respective control are marked; as derived from statistical analysis using two-way ANOVA followed by LSD.

| | Plant height (cm) | No. of leaves per plant | Plant fresh weight (g) | Plant dry weight (g) | No. of pods per plant | Pod length (cm) | Pod dry weight (g) | No. of seeds per plant |
|---|---|---|---|---|---|---|---|---|
| Biogenic | 23.33 | 18.00*** | 21.44* | 3.09 | 1.17 | 22.71*** | 1.13 | 12.00*** |
| | ±1.51 | ±2.68 | ±4.73 | ±1.29 | ±0.75 | ±3.45 | ±0.36 | ±4.24 |
| Chemogenic | 24.33 | 16.00 | 20.86* | 2.78 | 1.33**** | 21.13*** | 1.17 | 12.67*** |
| | ±3.67 | ±3.63 | ±4.63 | ±1.07 | ±0.82 | ±3.87 | ±0.34 | ±12.16 |
| Soluble P | 22.83 | 17.00**** | 18.84** | 2.56 | 1.33**** | 19.25 | 1.06 | 11.17**** |
| | ±2.56 | ±3.63 | ±4.11 | ±0.77 | ±0.82 | ±4.62 | ±0.39 | ±8.52 |
| Insoluble P | 20.50 | 14.00 | 12.03 | 1.46 | 0.67 | 16.50 | 0.82 | 6.50 |
| | ±2.07 | ±2.45 | ±3.08 | ±0.58 | ±0.52 | ±1.91 | ±0.11 | ±5.21 |
| Control | 21.33 | 13.50 | 12.77 | 1.58 | 0.50 | 15.33 | 0.69 | 5.33 |
| | ±1.51 | ±2.51 | ±2.66 | ±0.42 | ±0.55 | ±3.21 | ±0.26 | ±5.92 |

*For $P < 0.0001$.
**For $P < 0.001$.
***For $P < 0.01$.
****For $P < 0.05$.

100% (Cabeza et al., 2011). In the alkaline soil environment, its solubility is minimal at pH 9–11 (Degryse et al., 2017). Below pH 8, there is a striking increase in solubility with decreasing pH (Degryse et al., 2017). Hence, the lower soil pH promotes faster dissolution and accordingly increased P concentrations at the soil:struvite interface solution. In this experiment, the initial acidic soil pH in both the biogenic (4.98) and chemogenic systems (4.92) was found to be favorable for enhanced solubilization of struvite and subsequent release of nitrogenous nutrients, which resulted in higher $NO_3$–N and $NH_4$–N concentrations in those system (Siciliano, 2015). Similar observations on phosphorus use efficiency in struvite were made by Vaneeckhaute et al. (2016) when comparing struvite against other biobased fertilizers and TSP tested in acidic sandy soils: P availability and uptake by *Zea mays* (maize) were observed to be high.

At the initial stage, the concentration of available-P in soil was significantly higher in the SP (8.06 mg $kg^{-1}$) than all other systems tested because it was treated with $K_2HPO_4$ that served as a ready source of soluble phosphate (Fig. 5e). Bg and Cg were treated with struvite, a slow release phosphatic fertilizer, and IP received insoluble phosphate. During the middle and end of the study, available P concentrations in treatments Bg (3.45 and 4.45 mg $kg^{-1}$) and Cg (4.03 and 4.33 mg $kg^{-1}$) were significantly higher than in the other treatments because the release of phosphate was sustained under acidic soil pH range for those systems treated with struvite, essentially acting as a slow release fertilizer. Siciliano (2015) reported that the struvite has the potential to increase available P, $NO_3$–N and $NH_4$–N in soil. As the plants grow, they utilize available nutrients from soil, causing a gradual decrease in $NO_3$–N, $NH_4$–N and available P.

Both acid and alkaline phosphatase activity increased with increasing time (Fig. 5g & h), with available-P increasing more at the end point than that in the mid-point in all systems. Similar time-dependent phosphatase activity was reported by other researchers (Bastida et al., 2019). With plant growth, microbial population in the rhizosphere increased, exhibiting higher acid phosphatase activity till the plants attained maturity (Holz et al., 2020). Contrarily, alkaline phosphatase activity did not vary significantly in all treatments up to day 30; thereafter such activity increased significantly with increase in soil pH. Available phosphate concentrations were found to be negatively correlated ($R^2 = 0.756$ to 0.889) with acid phosphatase activity whereas no relation was found with alkaline phosphatase activities. This implies that enzymatic P transformation was controlled by the prevailing pH regime of the soil (Bastida et al., 2019).

Increased plant growth and number of seeds produced per plant were observed in biogenic, chemogenic and soluble P systems (Table 4) where phosphatic nutrient was adequately available. Similar observations were reported for Chinese flowering cabbage (*Brassica parachinensis*), Chinese chard (*Brassica rapa* var. *chinensis*), water spinach (*Ipomoea aquatica*) and water convolvulus (*Ipomea aquatica, I. reptans*) by Li and Zhao (2003), Chinese cabbage by Ryu et al. (2012), and spinach (*Spinacia oleracea*) by Siciliano (2015).

The systems which received biogenic and chemogenic struvite revealed significantly better plant growth promotion traits, including plant height, fresh weight, dry weight, pod length and number of seeds per plant (Table 4). This has significant implication for potential application of struvite in agriculture for cultivation of cowpea plant. Several researchers reported such increase in biomass and yield in struvite treated system related to external factors, such as the long-lasting availability of nutrients and the reaction with the binding sites, while working with struvite derived from semiconductor wastewater (Ryu et al., 2012), methanogenic landfill leachate (Siciliano, 2015) and industrial wastewater (El Diwani et al., 2007).

Compared to the treatment involving insoluble P (IP), the struvite treated systems (Cg and Bg) had a greater amount of both available P and N showing their higher fertilizer mineralization potential. The phosphate mineralization indexes of different treatments showed that P mineralization was maximum in SP (0.057) and the least in IP (0.006). Struvite treated systems with moderate PMI (Bg: 0.016; Cg: 0.017) indicated that both biogenic and chemogenic struvite served as slow

release fertilizer, which offered 28%–30% slower rate of mineralization than that in $KH_2PO_4$ - an easily soluble phosphatic fertilizer, which can be corroborated with findings of Talboys et al. (2016).

The chlorophyll content in plants grown in both systems spiked with biogenic and chemogenic struvite can be justified by additional supplementation of Mg to those soils through struvite solubilization. Magnesium has an important role in the synthesis of chlorophyll and phosphorylating enzyme (Li and Zhao, 2003; Ryu et al., 2012).

At the end of the mesocosm plant growth trial, ammonium concentrations were recorded at higher levels compared to diminished levels of nitrate particularly in the struvite supplemented treatments. The correlation between ammonium and nitrate concentration showed that although a strong positive correlation was established in all treatments, struvite treated systems reflected relatively lower $R^2$ values (Bg: 0.914; Cg: 0.92) over others (SP: 0.987; IP: 0.995; C: 0.988) [Supplementary Information], showing weakening of nitrification in the former treatments. This is a positive aspect because nitrate can be easily leached through the soil. This observation is corroborated by several studies which recorded superior growth qualities of vegetables grown in struvite supplemented pots compared to the pots without any extraneous input of N and P (El Diwani et al., 2007; Ryu et al., 2012). Although the soil used in the study is reported to be rich in nitrogen but deficient in phosphorus (Chatterjee et al., 2015; Pati et al., 2016). Besides the used variety of leguminous plant species (*Vigna unguiculata*, variety: BCCP-3) can fix N but need high amount of P which need to be supplied through extraneous input. Therefore, any treatment with extraneous input of N was avoided. The real difference in fertilizer value between struvite and a typical commercial fertilizer was not much reflected due to the fact that although rate of solubilization of phosphate was more in case of the SP ($KH_2PO_4$) compared to biogenic and chemogenic struvite, all concentrations might have satisfied the plant's demand. On the other hand, more leaching of soluble phosphate in case of SP might have been reflected in its realized productive performance.

Many reported struvite mineralization processes (Ryu et al., 2012; Sinha et al., 2014; Kabdaşlı and Tünay, 2018; Patel et al., 2020) are costly and energy intensive, requiring additional Mg sources, aeration, agitation and filtration. Contrarily, the biogenic synthesis process in this study did not require any additional Mg sources, and both the biogenic and chemogenic syntheses were conducted as static batch process in the absence of aeration, agitation and filtration steps.

## 4. Conclusions

This study showed that the nutrients present in HU can be recovered as biofertilizer (struvite) following chemogenic and biogenic routes. Both treatments with chemogenic and biogenic struvite stimulated plant growth comparable to treatment with inorganic soluble phosphate, and significantly better than the unfertilized control and insoluble phosphate treatments. The nitrogen-rich but phosphorus-deficient soil, and nitrogen-fixing but high phosphorus demanding variety of leguminous plant species (*Vigna unguiculata*, variety: BCCP-3) used in this study confirmed that the chief nutrient responsible for plant growth promoting potentials of the tested biominerals was phosphorus. The chemogenic and biogenic struvite acted as slow release fertilizer sustaining nutrient supply and averting unwanted nutrient leaching during the growth of the plant. The 15 years old struvite passing through a natural aging process was found to lose $NH_4^+$, but retained $PO_4^{3-}$ and $Mg^{2+}$, which implied that the biofertilizer could retain its phosphate fertilizing potential for a longer period than its N fertilizing capacity.

When converting HU to biofertilizer ('waste into wealth'), struvite production was higher in the chemogenic process using magnesia (474 $\pm$ 9.64 mg $L^{-1}$) than the biogenic mode (345 $\pm$ 6.08 mg $L^{-1}$) employing *Pseudomonas aeruginosa* KUJM KY355382.1. However, the latter process should be preferred owing to its eco-friendly nature. For successful attainment of the circular economic objectives, the microbe-mediated 'waste to wealth' valorization protocol needs to be optimized. Nonetheless, it warrants further follow-up studies under real world situations after optimizing and up-scaling the bacterial struvite production system. In future research, the fertilizer potential of the biogenic struvite should be tested on different soils and in different agro-climatic soil environments, which will help translate the laboratory scale microcosm and outdoor mesocosm findings at field scale, and endure their reality check, successful replication, adequate reliability and adaptation of the technology. The acid test is its translation from 'lab to land' level through commercialization and down-to-earth application as an integral part of the systematic agricultural management strategy.

## CRediT authorship contribution statement

**Jayanta Kumar Biswas:** Conceptualization, Funding acquisition, Investigation, Project administration, Supervision, Methodology, Writing – original draft, Writing – review & editing, Software, Validation. **Monojit Mondal:** Conceptualization, Data curation, Formal analysis, Methodology, Software, Validation, Writing – original draft. **Dhrubajyoti Majumdar:** Data curation, Formal analysis, Methodology, Software. **Amit Bhatnagar:** Writing – review & editing. **Binoy Sarkar:** Writing – review & editing, Validation. **Meththika Vithanage:** Writing – review & editing, Validation. **Erik Meers:** Writing – review & editing, Validation. **Filip M.G. Tack:** Writing – review & editing, Validation. **Deepak Pant:** Writing – review & editing. **Ramesh Goel:** Writing – review & editing.

## Declaration of competing interest

The authors declare that they have no known competing financial interests or personal relationships that could have appeared to influence the work reported in this paper.

## Acknowledgments

The authors are grateful to the University of Kalyani for providing funding (No. 1R/URS/EnvMangt/2013) and all infrastructural and analytical support for carrying out the research. They also acknowledge some instrumental and analytical facilities for the present study received under University of Kalyani's scheme "Promotion of University Research and Scientific Excellence" (PURSE) sponsored by the Department of Science & Technology (DST), Government of India.

## Appendix A. Supplementary data

Supplementary material related to this article can be found online at https://doi.org/10.1016/j.eti.2021.102152. E-supplementary data of this work can be found in online version of the paper.

## References

Abbona, F., Lundager, M.H.E., Boistelle, R., 1982. Crystallization of two magnesium phosphates: struvite and newberite: effects of pH and concentration. J. Cryst. Growth 57, 6–14.

Angoni, K., Popp, J., Kiefe, W., 1998. A vibrational spectroscopy study of urinary sand. Spectrosc. Lett. 31, 1771–1782. http://dx.doi.org/10.1080/00387019808007453.

Bastida, F., Jehmlich, N., Martínez-Navarro, J., Bayona, V., García, C., Moreno, J.L., 2019. The effects of struvite and sewage sludge on plant yield and the microbial community of a semiarid Mediterranean soil. Geoderma 337, 1051–1057.

Bhattacharya, A., Naik, S.N., Khare, S.K., 2018. Harnessing the bio-mineralization ability of urease producing *Serratia marcescens* and *Enterobacter cloacae* EMB19 for remediation of heavy metal cadmium (II). J. Environ. Manag. 215, 143–152.

Biswas, J.K., Mondal, M., Rinklebe, J., Sarkar, S.K., Chaudhuri, P., Rai, M., Shaheen, S.M., Song, H., Rizwan, M., 2017. Multi-metal resistance and plant growth promotion potential of a wastewater bacterium *Pseudomonas aeruginosa* and its synergistic benefits. Environ. Geochem. Health 39 (6), 1583–1593.

Biswas, J.K., Rana, S., Meers, E., 2020. Bioregenerative nutrient recovery from human urine: Closing the loop in turning waste into wealth. In: Meers, E., Velthof, G., Michels, E., Rietra, R. (Eds.), Biorefinery of Inorganics: Recovering Mineral Nutrients from Biomass and Organic Waste. John Wiley & Sons, pp. 161–176.

Bradenburg, K., 2005. Diamond, Ver. 3.1eM. Crystal Impact GbR, Bonn, Germany.

Cabeza, R., Steingrobe, B., Römer, W., Claassen, N., 2011. Effectiveness of recycled P products as P fertilizers, as evaluated in pot experiments. Nutr. Cycl. Agroecosyst. 91 (2), 173–184.

Cahil, A., Najdoski, M., Stefov, V., 2007. Infrared and Raman spectra of magnesium ammonium phosphate hexahydrate (struvite) and its isomorphous analogues. IV. FTIR spectra of protiated and partially deuterated nickel ammonium phosphate hexahydrate and nickel potassium phosphate hexahydrate. J. Mol. Struct. 834, 408–413.

Carstea, E.M., Bridgeman, J., Baker, A., Reynolds, D.M., 2016. Fluorescence spectroscopy for wastewater monitoring: a review. Water Res. 95, 205–219.

Chatterjee, S., Santra, P., Majumdar, K., Ghosh, D., Das, I., Sanyal, S.K., 2015. Geostatistical approach for management of soil nutrients with special emphasis on different forms of potassium considering their spatial variation in intensive cropping system of West Bengal, India. Environ. Monit. Assess. 187 (4), 1–17.

Chojnacka, K., Moustakas, K., Witek-Krowiak, A., 2020. Bio-based fertilizers: A practical approach towards circular economy. Bioresour. Technol. 295, 122223.

Degryse, F., Baird, R., da Silva, R.C., McLaughlin, M.J., 2017. Dissolution rate and agronomic effectiveness of struvitefertilizers – effect of soil pH, granulation and base excess. Plant Soil 410 (1–2), 139–152.

Dolomanov, O.V., Bourhis, L.J., Gildea, R.J., Howard, J.A., Puschmann, H., 2009. OLEX2: a complete structure solution, refinement and analysis program. J. Appl. Crystallogr. 42 (2), 339–341.

El Diwani, G., El Rafie, S., El Ibiari, N.N., El-Aila, H.I., 2007. Recovery of ammonia nitrogen from industrial wastewater treatment as struvite slow releasing fertilizer. Desalination 214 (1–3), 200–214.

Ferraris, G., Fuess, H., Joswig, W., 1986. Neutron diffraction study of $MgNH_4PO_4 \cdot 6H_2O$ (struvite) and survey of water molecules donating short hydrogen bonds. Acta Crystallogr. B 42, 253–258.

Fridgen, J.L., Varco, J.J., 2004. Dependency of cotton leaf nitrogen, chlorophyll, and reflectance on nitrogen and potassium availability. Agron. J. 96 (1), 63–69.

Frost, R.L., Weier, M.L., Martens, W.N., Henry, D.A., Mills, S.J., 2005. Raman spectroscopy of newberyite, hannayite and struvite. Spectrochim. Acta A 62, 181–188.

Gherghel, A., Teodosiu, C., De Gisi, S., 2019. A review on wastewater sludge valorisation and its challenges in the context of circular economy. J. Clean. Prod. 228, 244–263.

Gonzalez-Martinez, A., Leyva-Díaz, J.C., Rodriguez-Sanchez, A., Munoz-Palazon, B., Rivadeneyra, A., Poyatos, J.M., Martinez-Toledo, M.V., 2015. Isolation and metagenomic characterization of bacteria associated with calcium carbonate and struvite precipitation in a pure moving bed biofilm reactor-membrane bioreactor. Biofouling 31 (4), 333–348.

González-Muñoz, M.T., Rodriguez-Navarro, C., Martínez-Ruiz, F., Arias, J.M., Merroun, M.L., Rodriguez-Gallego, M., 2010. Bacterial biomineralization: new insights from myxococcus-induced mineral precipitation. Geol. Soc. Spec. Publ. 336 (1), 31–50.

Holz, M., Zarebanadkouki, M., Carminati, A., Becker, J.N., Spohn, M., 2020. The effect of root hairs on rhizosphere phosphatase activity. J. Plant. Nutr. Soil Sci. 183 (3), 382–388.

Kabdaşlı, I., Tünay, O., 2018. Nutrient recovery by struvite precipitation, ion exchange and adsorption from source-separated human urine–a review. Environ. Technol. Rev. 7 (1), 106–138.

Keeney, D.R., Nelson, D.W., 1982. Nitrogen-inorganic forms. In: Page, A.L., Miller, R.H., Keeney, D.R. (Eds.), Methods of Soil Analysis Part 2 Chemical and Microbiological Properties, second ed. ASA and SSSA, Madison, pp. 643–698.

Li, X.Z., Zhao, Q.L., 2003. Recovery of ammonium-nitrogen from landfill leachate as a multi-nutrient fertilizer. Ecol. Eng. 20, 171–181.

Olsen, S.R., Cole, C.V., Watanabe, F.S., Dean, L.A., 1954. Estimation of available phosphorus in soils by extraction with sodium bicarbonate. In: Circular 939. United States Department of Agriculture, Washington DC.

Onchoke, K.K., Franclemont, C.M., Weatherford, P.W., 2018. Structural characterization and evaluation of municipal wastewater sludge (biosolids) from two rural wastewater treatment plants in East Texas, USA. Spectrochim. Acta A 204, 514–524.

Pandorf, M., Hochmuth, G., Boyer, T.H., 2018. Human urine as a fertilizer in the cultivation of snap beans (*Phaseolus vulgaris*) and turnips (*Brassica rapa*). J. Agric. Food Chem. 67 (1), 50–62.

Patel, A., Mungray, A.A., Mungray, A.K., 2020. Technologies for the recovery of nutrients, water and energy from human urine: A review. Chemosphere 2020, 127372.
Pati, S., Pal, B., Badole, S., Hazra, G.C., Mandal, B., 2016. Effect of silicon fertilization on growth, yield, and nutrient uptake of rice. Commun. Soil Sci. Plant Anal. 47 (3), 284–290.
Piotrowska-Długosz, A., Wilczewski, E., 2014. Soil phosphatase activity and phosphorus content as influenced by catch crops cultivated as green manure. Pol. J. Environ. Stud. 23 (1), 157–165.
Pratt, C., Parsons, S.A., Soares, A., Martin, B.D., 2012. Biologically and chemically mediated adsorption and precipitation of phosphorus from wastewater. Curr. Opin. Biotechnol. 23, 890–896.
Rana, S., Biswas, J.K., Rinklebe, J., Meers, E., Bolan, N., 2017. Harnessing fertilizer potential of human urine in a mesocosm system: a novel test case for linking the loop between sanitation and aquaculture. Environ. Geochem. Health 39 (6), 1545–1561.
Ravndal, K.T., Opsahl, E., Bagi, A., Kommedal, R., 2018. Wastewater characterisation by combining size fractionation, chemical composition and biodegradability. Water Res. 131, 151–160.
Robles, Á., Aguado, D., Barat, R., Borrás, L., Bouzas, A., Giménez, J.B., Martí, N., Ribes, J., Ruano, M.V., Serralta, J., Ferrer, J., 2020. New frontiers from removal to recycling of nitrogen and phosphorus from wastewater in the Circular Economy. Bioresour. Technol. 300, 122673.
Ryu, H.D., Lim, C.S., Kang, M.K., Lee, S.I., 2012. Evaluation of struvite obtained from semiconductor wastewater as a fertilizer in cultivating Chinese cabbage. J. Hazard. Mater. 221–222, 248–255.
Sheldrick, G.M., 1996. SADABS: Software for Empirical Absorption Correction, Vol. 4. University of Gottingen, Institut fur Anorganische Chemieder Universitat, Tammanstrasse, pp. 1999–2003.
Sheldrick, G.M., 2001. SHELXTL, a Software for Empirical Absorption Correction Ver. 6.12. Bruker AXS Inc., WI, Madison.
SHELXTL, 2000. Reference Manual, Ver. 6.1. Bruker Analytical X-ray Systems, Inc., WI, Madison.
Siciliano, A., 2015. Assessment of fertilizer potential of the struvite produced from the treatment of methanogenic landfill leachate using low-cost reagents. Environ. Sci. Pollut. Res. 23 (6), 5949–5959.
Simha, P., Zabaniotou, A., Ganesapillai, M., 2018. Continuous urea–nitrogen recycling from human urine: A step towards creating a human excreta based bio–economy. J. Clean. Prod. 172, 4152–4161.
Sinha, A., Singh, A., Kumar, S., Khare, S.K., Ramanan, A., 2014. Microbial mineralization of struvite: a promising process to overcome phosphate sequestering crisis. Water Res. 54, 33–43.
SMART & SAINT, 2003. Software Reference Manuals, Version 6.45. Bruker Analytical X-ray Systems, Inc., WI, Madison.
Soares, A., Veesam, M., Simoes, F., Wood, E., Parsons, S.A., Stephenson, T., 2013. Biostruvite: a new route to recover phosphorus from wastewater. CLEAN–Soil Air Water 7, 994–997.
Stefov, V., Abdija, Z., Najdoski, M., Koleva, V., Petruševski, V.M., Runčevski, T., Dinnebier, R.E., Šoptrajanov, B., 2013. Infrared and Raman spectra of magnesium ammonium phosphate hexahydrate (struvite) and its isomorphous analogues. IX: Spectra of protiated and partially deuterated cubic magnesium caesium phosphate hexahydrate. Vib. Spectrosc. 68, 122–128.
Tabatabai, M.A., Bremner, J.M., 1969. Use of p-nitrophenyl phosphate for assay of soil phosphatase activity. Soil Biol. Biochem. 1 (4), 301–307.
Talboys, P.J., Heppell, J., Roose, T., Healey, J.R., Jones, D.L., Withers, P.J., 2016. Struvite: a slow-release fertiliser for sustainable phosphorus management? Plant Soil 401 (1–2), 109–123.
Trobajo, C., Salvadó, .M.A., Pertierra, P., Alfonso, B.F., Blanco, J.A., Khainakov, S.A., García, J.R., 2007. Synthesis, structure and magnetic characterization of two phosphate compounds related with the mineral struvite: KNiPO4 $\mu \cdot \mu$6H2O and $NaNiPO_4\mu \cdot \mu 7H_2O$. Z. Anorg. Allg. Chem. 633 (11–12), 1932–1936.
Uysal, A., Yilmazel, Y.D., Demirer, G.N., 2010. The determination of fertilizer quality of the formed struvite from effluent of a sewage sludge anaerobic digester. J. Hazard. Mater. 181 (1–3), 248–254.
Vaneeckhaute, C., Janda, J., Vanrolleghem, P.A., Filip, M.G., Meers, E., 2016. Phosphorus use efficiency of bio-based fertilizers: Bioavailability and fractionation. Pedosphere 26 (3), 310–325.
Weil, M., 2008. The struvite-type compounds $M$ $[Mg(H_2O)_6](XO_4)$, where $M$ = Rb, Tl and $X$ = P, As. Cryst. Res. Technol. 43 (12), 1286–1291.
Yang, H., Martinelli, L., Tasso, F., Sprocati, A.R., Pinzari, F., Liu, Z., Downs, R.T., Sun, H.J., 2014. A new biogenic, struvite-related phosphate, the ammonium-analog of hazenite, $(NH_4)NaMg_2(PO_4)_2 \cdot 14H_2O$. Am. Mineral. 99, 1761–1765.